

C.P. No. 989

R 35876

C.P. No. 989



MINISTRY OF TECHNOLOGY

AERONAUTICAL RESEARCH COUNCIL

CURRENT PAPERS

The Local Pressure Field of Turbulent Jets

By

P. O. A. L. Davies, N. W. M. Ko and B. Bose

LONDON: HER MAJESTY'S STATIONERY OFFICE

1968

PRICE SIX SHILLINGS NET

R 35876

R 35876

10. 11. 19

May, 1967

The Local Pressure Field of Turbulent Jets
-By-
P. O. A. L. Davies, N. W. M. Ko and B. Bose,
University of Southampton



SUMMARY

The characteristics of the pressure field associated with the turbulent shear flows of a jet have been studied in some detail. Components of the field in the potential core appear to be moving with a phase velocity equal to the local speed of sound in directions roughly normal to the shear layer. Some components of the hot wire signal can be associated with the jet structure as a single complex source while others are related to the local characteristics of the turbulence.

An estimate of the strength of the fluctuating pressure field throughout the whole region of the jet flow is presented.

Introduction

A knowledge of the fundamental mechanisms of noise generation is of particular interest in the development of technology for reducing jet noise. The mechanism by which turbulence produces noise is now on a sound theoretical basis following the work of Lighthill^{1,2} and others³, and the theory accounts for the general characteristics of noise from jets in terms of dimensionless arguments. Calculations of the observed characteristics of the radiated jet noise field cannot yet be performed with available measurements of turbulent structure, simply because the flow characteristics required by the theory have been too difficult to measure. A major discrepancy in the existing knowledge therefore concerns the relation between the sound generated per unit volume of turbulence and the leading jet flow characteristics that can be conveniently measured at present^{2,3}. A possible experimental method for assessing the source strength distribution has been suggested by Morfey⁴ and involves measuring the covariance between the pressure and the radial velocity fluctuations.

Considerable progress has been made in describing the structure of the jet turbulence in terms of the statistical properties of the velocity fluctuations measured with a hot wire^{5,6,7}. However, very little information exists concerning the pressure fluctuations associated with the turbulence, chiefly due to the practical difficulties of measuring the

pressure/

* Replances A.R.C.29 065.

pressure fluctuations. This seems to be the chief experimental problem in making measurements that will yield the source strength distributions directly, using Morfey's theory. A preliminary survey⁸ provided enough experimental evidence to suggest that the problem of pressure measurement in high speed flow might be resolved, for the jet at least. More evidence is presented here which supports this conclusion.

The method is based on the well established fact that the hot wire measures the instantaneous local mass flux (ρv). This means that the fluctuating hot wire signal consists of two components, one from density and one from velocity fluctuations. At the moderate mean flow Mach numbers of most of the measurements, it has been justly argued that density fluctuations must be negligible compared with those in velocity, so one is justified in ignoring the contribution from the density perturbations. Such an assumption, however, ignores the strong local accelerations produced by interactions within the eddies and the potential field produced by the vorticity fluctuations. Within the turbulence, the local density fluctuations would still be relatively small, but it is shown later that it is not reasonable to ignore them altogether.

It is convenient to consider the problem in terms of the known structure of the jet. This provides three natural divisions, the high speed potential core where the velocity fluctuations are small, the turbulent mixing region where velocity fluctuations are dominant and the external entrainment region where the velocity is low enough to permit the use of a microphone for the measurements. Evidence will also be presented linking the measurements in these regions, demonstrating they describe a continuous field.

Apart from the results reported here, other near field measurements^{6,9,10} have been made with a microphone just outside the jet. Unfortunately most of the results are confined to directivity patterns and spectra and do not include intensity measurements. The spectra all exhibit a pronounced peak and about 90% of the signal energy is contained within the band one octave each side of the peak frequency f . In addition, most of the published measurements of Strouhal number fD/U_0 where D is the jet diameter and U_0 the jet velocity are in fair agreement with each other.

If we take a typical measurement, we find the value of the Strouhal number just outside the jet, two diameters downstream say, is about 0.4. The width of the turbulent mixing region δ is about $0.5D$ at this point. The wavelength λ of the near field will be of the order of c/f , where c is the local speed of sound. Hence the ratio of the wavelength of the pressure field to the width of the mixing region is given by

$$\frac{\lambda}{\delta} = \frac{5}{M_0},$$

where M_0 is the jet Mach number. It is easily shown that, in fact this ratio remains constant for the first five diameters of the jet flow, since

the/

the Strouhal number measured at the jet is inversely proportional to the distance downstream, while the width of the mixing region is directly proportional to this distance. We can expect therefore that the fluctuating pressure field will remain correlated over much greater distances than the velocity fluctuations.

Similar cold air jets one and two inches in diameter were used for the measurements, with flow speeds up to a Mach number of 0.5. The new measurements include spectra, cross-correlations and intensity of the hot wire and microphone signals. Measurements in the potential core are reported first and the near field measurements appear last. Analysis of the results is concerned mainly with describing the characteristics of the pressure field within and surrounding the jet.

A diagram of the two jets appears in Fig. 1. The settling chambers include acoustic treatment to minimise standing waves and absorb the noise generated by the flow control valves. The acoustic treatment was efficient enough to suppress standing waves in the jet flow. These were most apparent with an untreated expansion chamber just downstream of the jet exit where the existence of discrete tones has been reported by some observers. These may be related to broad vortex rings at the jet orifice that appear in Schlieren pictures reported in Ref. 6 or as local waves in the level of the velocity fluctuations¹¹. However, careful measurements by Wilkinson¹² show that any measurable initial vortex pattern is probably related to acoustic conditions in the stilling chamber, and does not exist when the upstream influence is removed. The effects, if present, are most readily discerned at low jet flow speeds.

The major features of jet structure are illustrated in Fig. 2. The boundaries of the potential core and mixing region are not sharply defined as suggested in the figure but exhibit a high degree of intermittency. This gives rise, as far as time averaged measurements are concerned, to a gradual merging from one region to another. The details of the structure are similar for both jets and represent universal jet behaviour. Many statistical properties of the velocity field exhibit strong similarity, provided their radial distribution is presented in space co-ordinates centred on the cylinder defined by the axial extension of the jet outlet. The results will therefore be presented in radial co-ordinates η , which is the tangent of the angle of the ray through the point subtended from the jet lip, i.e., $\eta = (Y - D/2)/X$.

2.1 Hot wire measurements

Typical power spectral density distributions of the hot wire signals appear in Fig. 3. The peaked spectrum was invariably found in the potential core or for the whole region where the value of the co-ordinate η is less than -0.1. The flat-topped spectra are typical of the signals obtained throughout the turbulent mixing region, over the range of co-ordinates $-0.1 < \eta < 0.25$. The rms value of the hot wire signals rises fairly rapidly over the first two diameters axially from the jet exit but then remains constant along lines of constant η .

Considering first the more peaked spectra, one can easily establish that more than 90% of the signal energy is concentrated around the peak frequency f . In the potential core of both jets it was found that, at constant

Mach/

Mach number, the Strouhal number based on this peak frequency remained almost constant beyond the first two diameters and its value was about the same for both jets. Towards the jet exit, where both the relative strength of the peak and the overall signal strength fell, the Strouhal number rose to another constant value about 20% higher than the downstream one. This behaviour is illustrated in Fig. 4. On the other hand, there does seem to be a slow systematic increase in Strouhal number with Mach number in subsonic flow and this is illustrated in Fig. 5.

It is now well known that the propagation of disturbances in the turbulent mixing region is dispersive¹³, and that high frequency components appear to travel faster than low frequency ones. Measurements of the convection speed of the disturbances in the potential core show that they are much less dispersive, (i.e., the cross-correlation decays slowly) than those in the mixing region. This result is probably not surprising since most of the energy is concentrated in a relatively narrow band of frequencies. The radial distribution of the axial convection speed appears in Fig. 6 and includes measurements made in both jets by some six different observers at Southampton and measurements by Bradshaw⁶. Although there is a fair degree of scatter among the measurements, the trend is fairly well established by the mean curve.

If one now measures the convection speed of a $\frac{1}{3}$ octave component of the signal centred at the peak of the potential core spectrum, one finds that the convection speed remains constant from the axis to the centre of the mixing region. The scatter of the individual measurements is now much smaller than those on Fig. 6, (i.e., is not more than 1 or 2%). This suggests that there is a coherent set of disturbances stretching right across the jet and running at the same speed as the strongest turbulence.

This evidence taken with the spectrum measurements all suggests that the hot wire signals do represent the combination of two components. A study of the probability distributions of the signals supports this view. Those in the potential core are Gaussian, while elsewhere the signals are not^{13,7}. Furthermore, if one examines the hot wire signals from the potential core and interprets them as velocity fluctuations, they always exceed $0.95 U_0$, which is far higher than their group velocity or the convection speed observed there. In fact they represent a disturbance travelling at the same speed as the most intense turbulence near $\eta = 0$. It seems plausible to assume that most of the signal energy in the potential core arises from the potential field of that part of the intense turbulence in the mixing region which also produces the external pressure field and the components of the radiated noise field.

The fact that this field stretches right across the jet from the potential core to the pressure field outside the jet is also indicated by cross-correlation measurements between a hot wire on the axis and one moved radially outwards. Typical measurements for one radial plane appear on Figs. 7 and 8. Again the behaviour observed was similar for both jets at corresponding axial positions down the jet. Within the potential core, up to the

inner/

inner edge of the mixing region the disturbances propagate radially with a phase velocity close to the local speed of sound. These regions are indicated by the cross hatching on Fig. 2. The signals just outside the mixing region are also quite well correlated with those in the potential core which suggests they also represent the same field. This provides further support to the suggestion that the signals in the potential core are density and velocity fluctuations associated with a "pressure" field threading right through the jet from the source regions in the turbulence.

One can estimate the phase velocity in the potential core since the signals there are mainly from one coherent field. It is not, however, possible to make this estimate with remainder of the results in Figs. 6 and 7 since strong signals from the turbulent velocity fluctuations are also present, and phase separation of the two components is no longer possible.

The above measurements do however provide enough information to make an estimate of the local strength of the potential field throughout the whole of the jet and its surroundings, and this will be performed in §3. Before doing so we shall examine the results of measurements of the near field just outside the mixing region.

2.2 Microphone measurements

The remainder of the experimental work reported here consisted of measurements of the field just outside the mixing region. The inner edge of this region was taken as a cone making an angle of 10° with the cylinder $\eta = 0$, and corresponds to a radial co-ordinate $\eta = 0.173$. Although the velocity here was small enough to permit the use of a microphone some precautions were necessary since its presence can disturb both the pressure field and the local flow. Initial measurements were therefore made with $\frac{1}{4}$ and $\frac{1}{2}$ in. Bruel and Kjaer microphones at points just outside the jet boundary. Careful comparison of the two sets of readings showed that both instruments gave the same output within 0.5 dB up to 1000 hertz and beyond this the spectra were almost exactly similar in shape but the output from the smaller microphone was 1 or 2 dB greater. Since microphone calibrations are not normally reliable to better than 0.5 dB, it was decided that measurements with the $\frac{1}{4}$ in. microphone would probably be as reliable as those with the special probe attachments, and that field interference effects were not serious.

The measured strength of the pressure field outside the jet appears in Fig. 9. It can be seen that there is little evidence of field distortions or standing waves in the measurements outside the majority of the jet. The radial plane containing the jet origin was, however, a reflecting surface (see Fig. 1) and although this was acoustically treated some distortion of the field close to it is present in the results.

The power spectra of the pressure field were all peaked, and very similar in shape. The Strouhal number of the pressure fluctuations was independent of jet Mach number over the speed range investigated. This can be seen in the typical normalised spectra plotted in Fig. 10. The increase in relative peak level indicated at the lower velocities vanished as the distance from the jet boundary increased.

The/

The value of the Strouhal number depends strongly on both the radial distance from the jet and the axial position. The axial variation along the ray $\eta = 0.173$ is illustrated in Fig. 11, where the dotted line has a slope -1 . Despite the scatter, the trends are clear and the results appear to form two groups dividing between $1 < X/D < 2$ as was found in the potential core. The radial variation of Strouhal number is plotted on Fig. 12. The interpretation of these results is difficult because they include the variation with axial displacement as well. However sets of measurements at constant axial distance can be distinguished and all show that the Strouhal number falls off radially, and the rate of fall tends to remain constant as one moves downstream. Careful analysis of individual runs suggests that the rate of fall-off is about half that in the axial direction. The results reported here compare fairly well with those from other observers^{6,9,10}.

Direct comparison between the potential core field and the estimated field on a Strouhal number basis is hardly practicable since they exhibit such differing distributions in space. This is clearly because a point pressure measurement represents the summation from the complex source distribution given by the whole jet, and this must necessarily be taken account of in any comparison.

3. Estimates of the pressure field strength from the measurements

(a) From spectrum measurements

The energy in any part of the turbulence spectrum can be calculated by subdividing it into a number of sections, where for any section we can represent the spectral density F_f by

$$F_f = F_o (f/f_o)^n .$$

Then the energy component of the entire spectrum lying between the two frequencies f_o and f_1 is given by

$$\begin{aligned} E_{o1} &= \int_{f_o}^{f_1} F_o \left(\frac{f}{f_o} \right) df \\ &= \frac{F_o f_o}{(n+1)} \left[\left(\frac{f}{f_o} \right)^{n+1} - 1 \right] \end{aligned}$$

provided n does not have the value -1 . If this is so the energy will become $F_o f_o \ln f_1/f_o$. Furthermore, provided n is less than -1 , the energy for the part of a spectrum extending towards infinite frequencies is always finite.

The/

The spectra measured in the potential core have a pronounced peak. The proportion of the energy contained in this peak can be found by finding the total spectral energy which is normally available as a direct measurement, and subtracting from it the energy of a flattened spectrum which excludes the peak. With reasonable care, the accuracy of the estimate of the proportion in the peak will be within 1 or 2% of its true value.

Assuming that the peak in this spectrum represents the contribution from the pressure or potential field while the background spectrum represents the turbulent velocity fluctuations, one can estimate the proportion of the total signal energy which is due to either disturbance. In the absence of significant temperature fluctuations, the hot wire signal will represent the instantaneous mass flux ρv . The rms time averaged fluctuating signal in the potential core will be the time average value $(\langle (\rho v - \rho_0 U_0)^2 \rangle)^{\frac{1}{2}}$, where U_0 is the jet exit velocity and ρ_0 the undisturbed density. The intensity I of the signal is defined as the normalised value of this quantity, or

$$I = \frac{(\langle (\rho v - \rho_0 U_0)^2 \rangle)^{\frac{1}{2}}}{\rho_0 U_0} .$$

This can be subdivided into turbulent and pressure field components I_t and I_p , making use of the relation

$$I^2 = I_t^2 + I_p^2 ,$$

provided the proportion of each component is known from the spectrum analysis.

Estimates of the pressure field intensity I_p at various positions in the potential core of both jets are given in table I. These have first been calculated from local intensity and spectrum measurements. The results indicate that the two jets have a different level of intensity in the potential core over the first two diameters of the flow. However, from this point downstream the intensity of the fluctuations is the same for both jets.

(b) From cross-correlation measurements

A second estimate of the value of the intensity I_p can be obtained from the radial cross-correlation measurements illustrated in Figs. 7 and 8. Within the potential core this should be obtained with good accuracy since we have already seen that the pressure signal is the dominant one there.

It has been demonstrated already that the hot wire signals come from two components in the flow, one due to the local density and velocity fluctuations associated with a pressure field and the other due to local turbulent velocity fluctuations. Furthermore it is possible to distinguish between these two components since the pressure disturbances will travel at the local acoustic velocity and this provides a fixed relationship between

their/

their length-scale and frequency. The turbulent velocity fluctuations are however directly associated with the local flow. These will also have a convection speed which provides a variable relationship between their length-scales and the frequency spectrum associated with them.

The convection speed of the velocity fluctuations increases with frequency in an apparently linear manner^{7,13}. The velocity field appears to behave in a non-frozen manner, i.e., decays in both space and time, while the pressure field more closely approximates a frozen one. Thus, although it is not possible to state definitely that a given element of signal at a given time is associated with the pressure or velocity field, one can make this distinction with regard to the time averaged statistical characteristics of the signal. The process of separating the two contributions is simplified by the fact that fluctuations due to the velocity field tend to remain correlated over much smaller distances than those associated with the pressure field.

Suppose the fluctuating component of the hot wire signal on the axis from the pressure field is A, while that from the local velocity fluctuations is b which is not coherent with A. A nearby radially positioned hot wire, at an appropriate time delay, will have a component of pressure signal kA, that is coherent with A, and a component B from local velocity fluctuations, which is not coherent with A. When the pressure field is dominant, the observed optimum cross-correlation between the signals will be

$$R_{\tau c} = \frac{(A + b)(kA + B)}{(A^2 + b^2 + k^2A^2 + B^2)^{\frac{1}{2}}}$$

$$= \frac{1}{\left[(1 + \alpha)(1 + \beta)^{\frac{1}{2}} \right]}$$

where $\alpha = b^2/A^2$ and $\beta = B^2/k^2A^2$. Since α is always small, this relation can be simplified to

$$R_{\tau c} = \frac{1 - \alpha/2}{(1 + \beta)^{\frac{1}{2}}}$$

If the hot wire signal representing the mean mass flux $\rho_o U_o$ is E, then the intensity of the second hot wire signal I will be given by

$$I^2 = \frac{(k^2A^2 + B^2)}{E^2},$$

while $I_p = (\langle (kA)^2 \rangle)^{\frac{1}{2}}/E$ and $I_t = (\langle B^2 \rangle)^{\frac{1}{2}}/E$, so that

$$I_p = (1 + \beta)^{\frac{1}{2}}I.$$

Noting/

Noting that, in the potential core $\alpha \approx \beta$, but also that a large enough wire separation can be obtained to make $\langle \varphi \rangle$ zero, we can find the value of $(1 + \beta)$ and α from the peaks of cross-correlation measurements. Thus we can determine I_p . In the mixing region where $\beta \gg 1$, the accuracy of the estimates of I_p will probably not be high.

The estimates of I_p from the cross-correlation measurements are also given in table I under the heading I_p' alongside the estimates of I_p from the spectra. The two sets agree quite well. To facilitate comparison the measurements in the potential core are plotted together in Fig. 13. The upper of the two curves is a good fit to eight of the ten sets of estimates of I_p , while the lower curve fits the other two. These are consistent with the systematic variations in signal strength that were noted close to the jet exit.

Since the agreement between the two estimates I_p and I_p' in the potential core are so close it seems reasonable to use the cross-correlation measurements to obtain a fair approximation to the remainder of the distribution across the mixing layer. These appear on Fig. 14 with the complete measured intensity profile. The results show that at $\eta = -0.1$ the contributions from the pressure and the velocity fluctuations are about equal. For larger values of η the velocity signals are the major component, while for smaller values of η they are the smaller one.

(c) Comparison with the external pressure field

The cross-correlation measurements extend to the region covered by the pressure measurements made with a microphone. For comparison, we need first to convert the pressure levels to equivalent hot wire intensity values. If we define the density and velocity fluctuations produced by the pressure field as ρ' and v' we have

$$\begin{aligned} (\rho v)_p &= (\rho_0 + \rho')(U + v') \\ &= \rho_0 U + \rho_0 v' + \rho' U, \end{aligned}$$

when we ignore second order quantities. Here U is the local mean velocity. For the fluctuating parts of the signal, we have, for plane waves,

$$\begin{aligned} \rho' U + \rho_0 v' &= \frac{p'}{c^2} U + \frac{p'}{c} \\ &= \frac{p'}{c} (1 + M) \end{aligned}$$

where p' is the fluctuating pressure and M is the local Mach number U/c . However

$$I_p^2 = \frac{\langle (\rho' U + \rho_0 v')^2 \rangle}{(\rho_0 U_0)^2},$$

so that the root mean pressure fluctuation is given by

$$\frac{(\langle p'^2 \rangle)^{\frac{1}{2}}}{p_o} = \frac{I_p \rho_o U_o c}{(1 + M)p_o}$$
$$= \frac{I_p \gamma M_o}{(1 + M)}$$

where γ is the ratio of the specific heats. Thus we can estimate I_p from the measured pressure level if the plane wave approximation for v' is valid. The isobars in Fig. 9 suggest that this assumption will not be too seriously in error. The estimates of I_p from the pressure field measurements appear low by a factor of about 3/2 in Fig. 14, so the agreement is reasonable. It represents a difference of about 2 dB in the pressure measurements.

3.1 Space correlation measurements

There is some further experimental evidence which supports the pressure intensity distribution on Fig. 14. Space correlations along lines of constant η should also provide some evidence of the coherent wave motion at large wire separations but the correlations will be very small. This is equivalent to using space separation as a filter to minimise the velocity fluctuations in comparison with the pressure field. With a new accurate and sensitive correlator it was possible to recover the very weak coherent signals at large separations and typical results appear in Fig. 15. These can then be easily transformed to spectra since the velocity is constant along lines of constant η . The result of doing so appears on Fig. 16. The spectrum near $\eta = 0$ should be compared with the spectrum at $Y/D = 0.5$ on Fig. 2. The reappearance of the peak in the spectrum is quite dramatic. The fact that it does not seem possible to recover the peak at larger values of η can be explained by the reduction of the strength of the pressure field and the limiting sensitivity of the correlator.

Discussion

The measurements have shown that a coherent pressure field, with a wavelength long compared with the thickness of the shear layers, extends from the jet axis to the near field outside the jet. The strength of this field is given to a fair approximation in Fig. 17. This provides a means of obtaining a direct indication of the fluctuating pressure within the mixing layer by using a hot wire placed on or near the jet axis and delaying the signal by an appropriate time.

This suggestion is now being used to estimate the strength of the noise sources in the jet by correlating this signal with the local radial velocity fluctuations. The measurements will be subject to give uncertainty as far as the absolute level of the covariance is concerned.

Since/

Since the pressure level estimates are probably close to the correct order of magnitude, the results can also be used to provide a standard of comparison for checking the performance of pressure transducers developed for use in high speed flow.

The results also suggest that the potential core and the highly sheared region surrounding it appear to behave like a broadly tuned acoustic resonator. At low flow speeds discrete frequencies have been associated with jet flow, however, it is likely that such discrete tones are associated with flow conditions in the stilling chamber upstream of the jet or with conditions at the jet lip.

The existence of two relatively uncorrelated signals near the inner edge of the mixing region provides an explanation for the discrepancy between the convection velocity observed there and that deduced from the skewness of the hot wire signals and the velocity there¹³. The skewness of these signals did account satisfactorily for the difference between the convection and mean velocity in the outer half of the mixing region. However, only about half the difference between mean and convection velocity at say $\eta = -0.1$ could be accounted for by skewness. The relative intensities of the pressure and velocity signals in this region has been plotted in Fig. 17, and it can be seen that they are almost equal. Since the axial convection velocity of the pressure field is just over $0.6 U_0$, half the signal energy must be travelling at this speed. This will then resolve the discrepancy noted above.

Acknowledgements

The authors wish to thank Prof. E. J. Richards, Mr. I. Wold and other members of the Institute for their advice and help. Thanks are also due to the Science Research Council, the British Council and the Ministry of Aviation for their interest and financial support and to UNESCO for Mr. Bose's Fellowship.

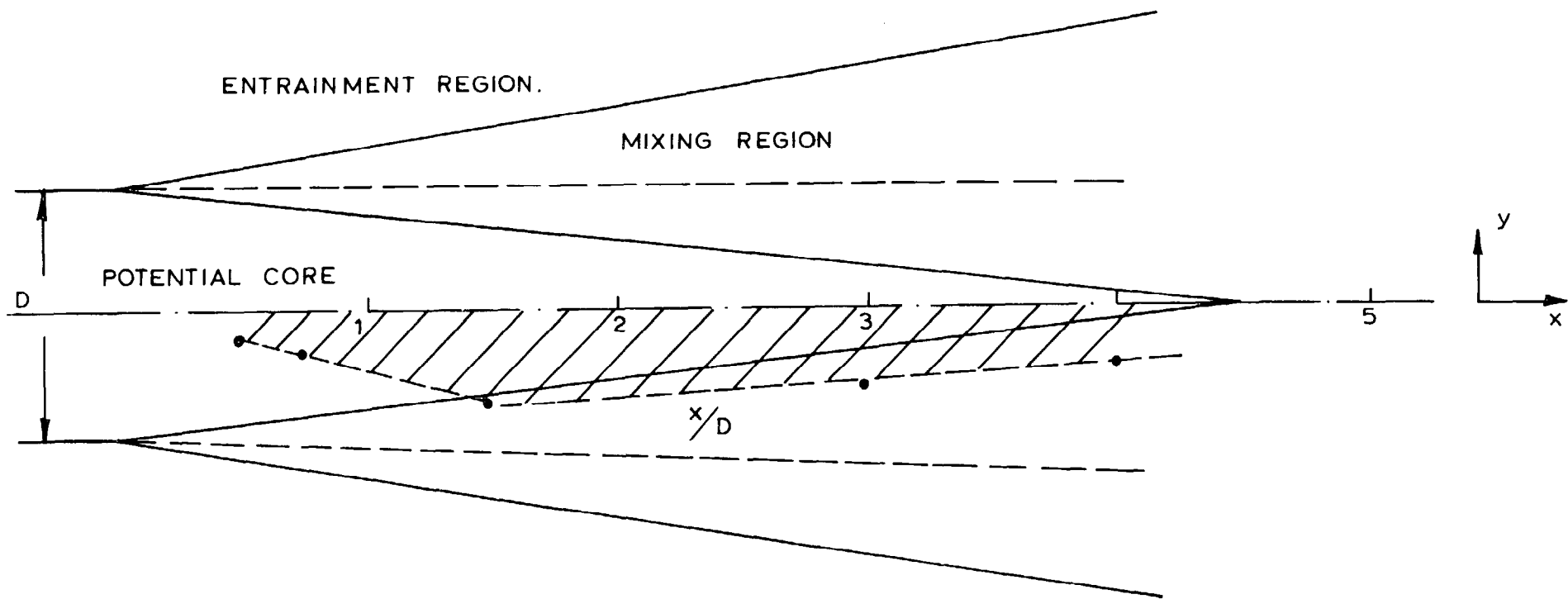
References/

References

- | <u>No.</u> | <u>Author(s)</u> | <u>Title, etc.</u> |
|------------|---|---|
| 1 | Lighthill, M. J. | On sound generated aerodynamically 1.
Proc. Roy. Soc. A 211, 1952, 564-587. |
| 2 | Lighthill, M. J. | Jet noise.
A.I.A.A. Journal 1, 1963, 1507-1517. |
| 3 | Ribner, H. S. | The generation of sound by turbulent jets.
Adv. App. Mech. 8, 1964, 103-182. |
| 4 | Morfey, C. L. | Sound fields and acoustic energy in
non-uniform flow.
Proc. 5th Int. Cong. Acoustics. Liège,
paper K15, September, 1965. |
| 5 | Davies, P. O. A. L.,
Fisher, M. J. and
Barrett, M. J. | Turbulence in the mixing region of a round
jet.
J. Fluid Mech. 15, 1963, 337-367. |
| 6 | Bradshaw, P.
Ferriss, D. H. and
Johnson, R. F. | Turbulence in the noise producing region of
a circular jet.
J. Fluid Mech. 19, 1964, 591-624. |
| 7 | Davies, P. O. A. L. | Turbulence structure in free shear layers.
A.I.A.A. Journal 4, 1966, 1971-1978. |
| 8 | Davies, P. O. A. L. and
Ko, N. W. M. | Near field generated by intense turbulence.
Proc. 5th Int. Cong. Acoustics, Liège
paper L53, September, 1965. |
| 9 | Mollo-Christensen, E. | Measurements of the near field pressure of
subsonic jets.
AGARD Rept. 449, April, 1963, <u>see also</u>
J. Fluid Mech. 8, 1960, 49-60 and J. Fluid
Mech. 18, 1964, 285-301. |
| 10 | Franklen, R. E. and
Foxwell, J. H. | Pressure fluctuations near a cold small-
scale air jet.
A.R.C. R. & M. 3162. May, 1958.
See also A.R.C. R. & M. 3161. June, 1958. |
| 11 | Bradshaw, P. | The effect of initial conditions on the
development of a free shear layer.
J. Fluid Mech. 26, 1966, 225-236. |
| 12 | Wilkinson, R. | An investigation of the turbulence near the
orifice of a 2 in. cold air jet. M.Sc.
Thesis, Southampton. February, 1966.
(Unpublished). |
| 13 | Fisher, M. J. and
Davies, P. O. A. L. | Correlation measurements in a non-frozen
pattern of turbulence.
J. Fluid Mech. 18, 1964, 97: 116. |

Table I
Estimates of I_p

Y/D	D = 1 in.				D = 2 in.				D = 1 in.				D = 2 in.				D = 2 in.											
	X/D = 1.5				X/D = 1.5				X/D = 3				X/D = 3				X/D = 4											
	I	I_p	I'_p		I	I_p	I'_p		I	I_p		I_p	I	I_p	I'_p		I	I_p		I_p	I	I_p	I'_p		I	I_p		I_p
0	0.0075	0.0073	-	0.0070	0.0065	-	0.019	0.0185	0.020	0.0185	-	0.020	0.0185	-	0.020	0.0185	0.031	0.0185	0.028	0.031	0.028	0.031	-	0.028	0.0185	0.031	0.028	0.031
0.05	0.0095	0.0089	0.0090	0.0077	0.0066	0.007	0.023	-	0.024	0.0207	0.021	0.024	0.0207	0.021	0.024	0.0355	0.0207	0.030	0.0355	0.030	0.0355	0.021	0.0207	0.0355	0.0207	0.0355	0.030	0.0355
0.1	0.0095	0.0089	0.0090	0.0092	0.007	0.0075	0.027	0.0225	0.028	0.0227	0.023	0.027	0.0227	0.023	0.028	0.043	0.0227	0.030	0.043	0.030	0.043	0.023	0.0227	0.043	0.0227	0.043	0.030	0.043
0.15	0.0146	0.0132	0.0126	0.0113	0.0087	0.009	0.033	-	0.034	0.0260	0.027	0.034	0.0260	0.027	0.034	0.051	0.0260	0.030	0.051	0.030	0.051	0.027	0.0260	0.051	0.0260	0.051	0.030	0.051
0.2	0.0146	0.0132	0.0126	0.0145	0.011	0.010	0.042	0.0280	0.044	0.0295	0.031	0.044	0.0295	0.031	0.044	0.051	0.0295	0.030	0.051	0.030	0.051	0.031	0.0295	0.051	0.0295	0.051	0.030	0.051
0.25	0.0267	0.0228	0.0226	0.0200	0.013	0.013	0.055	0.0280	0.057	0.0295	0.032	0.057	0.0295	0.032	0.057	0.051	0.0295	0.030	0.051	0.030	0.051	0.032	0.0295	0.051	0.0295	0.051	0.030	0.051
0.3	0.0267	0.0228	0.0226	0.028	0.018	0.017	0.070	0.070	0.073	0.024	0.024	0.073	0.024	0.024	0.073	0.051	0.024	0.030	0.073	0.030	0.073	0.024	0.024	0.073	0.024	0.073	0.030	0.073
0.35	0.071			0.043	0.019	0.018	0.070		0.091	0.019	0.018	0.091	0.019	0.018	0.091	0.051	0.019	0.030	0.091	0.030	0.091	0.018	0.018	0.091	0.018	0.091	0.030	0.091
0.4	0.071			0.072	0.019	0.012	0.070		0.110	0.019	0.012	0.110	0.019	0.012	0.110	0.051	0.019	0.030	0.110	0.030	0.110	0.012	0.012	0.110	0.012	0.110	0.030	0.110
0.45	0.125			0.108		0.010	0.070		0.122		0.010	0.122		0.010	0.122	0.051		0.030	0.122	0.030	0.122	0.010	0.010	0.122	0.010	0.122	0.030	0.122
0.50	0.125			0.130		0.008	0.070		0.131		0.008	0.131		0.008	0.131	0.051		0.030	0.131	0.030	0.131	0.008	0.008	0.131	0.008	0.131	0.030	0.131
0.55	0.127			0.131		0.006	0.070		0.132		0.006	0.132		0.006	0.132	0.051		0.030	0.132	0.030	0.132	0.006	0.006	0.132	0.006	0.132	0.030	0.132
0.60	0.106			0.110		0.0055	0.070		0.131		0.0055	0.131		0.0055	0.131	0.051		0.030	0.131	0.030	0.131	0.0055	0.0055	0.131	0.0055	0.131	0.030	0.131
0.70	0.045			0.046		0.003	0.070		0.111		0.003	0.111		0.003	0.111	0.051		0.030	0.111	0.030	0.111	0.003	0.003	0.111	0.003	0.111	0.030	0.111
0.80	0.017			0.018		0.0025	0.070		0.082		0.0025	0.082		0.0025	0.082	0.051		0.030	0.082	0.030	0.082	0.0025	0.0025	0.082	0.0025	0.082	0.030	0.082
0.90	0.006			0.007		0.002	0.070		0.045		0.002	0.045		0.002	0.045	0.051		0.030	0.045	0.030	0.045	0.002	0.002	0.045	0.002	0.045	0.030	0.045
1.00	0.006			0.005		0.002	0.070		0.045		0.002	0.045		0.002	0.045	0.051		0.030	0.045	0.030	0.045	0.002	0.002	0.045	0.002	0.045	0.030	0.045





 AREA OVER WHICH THE PHASE VELOCITY IN 'y' DIRECTION ATTAINS THE ORDER OF THE VELOCITY OF SOUND.

Fig. 2. Profile of the potential core of the jet.

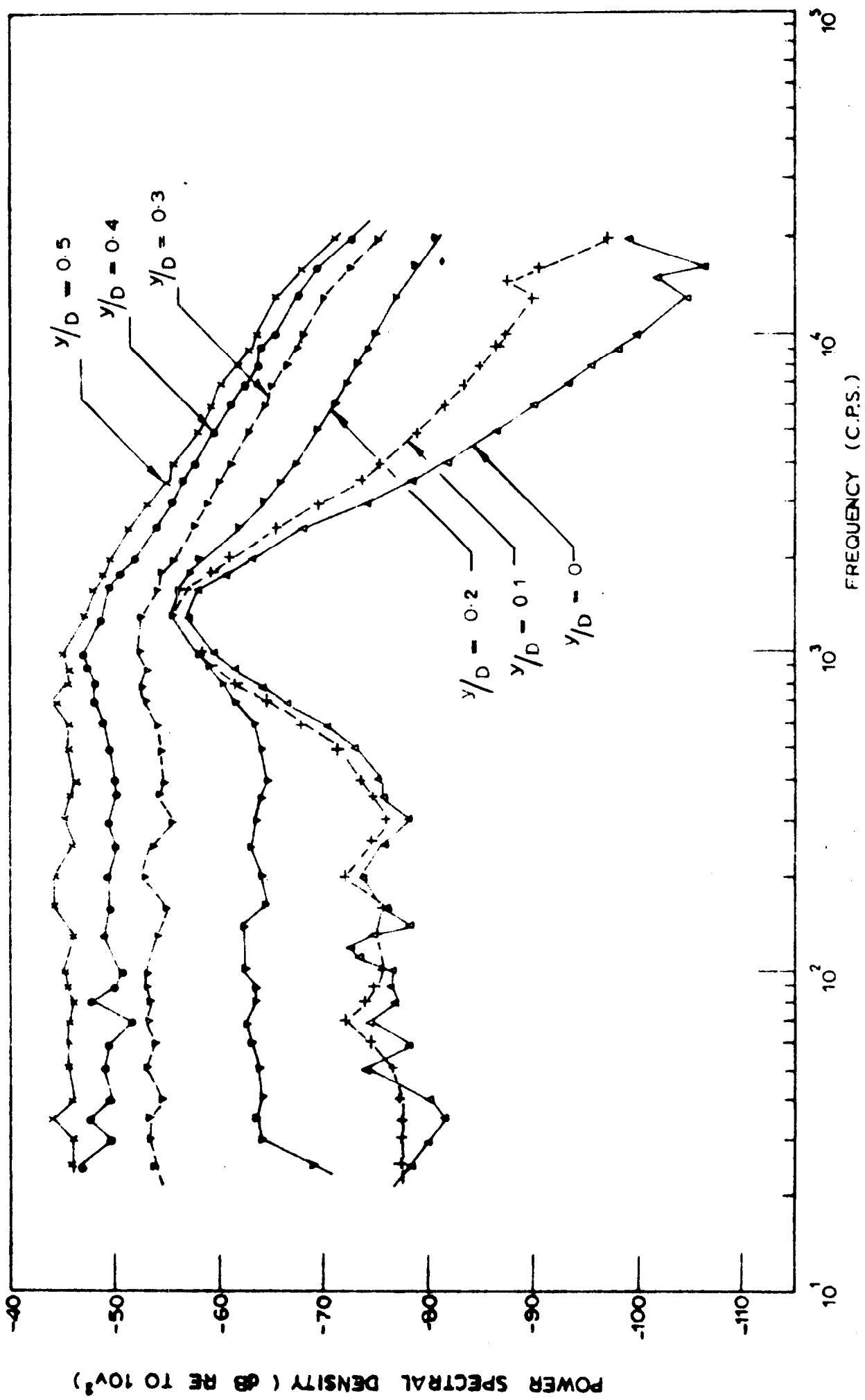


Fig 3 Power spectrum for different radial positions. Jet diameter - 1" $\bar{U}_0 = 245$ ft/sec $x/D = 3$

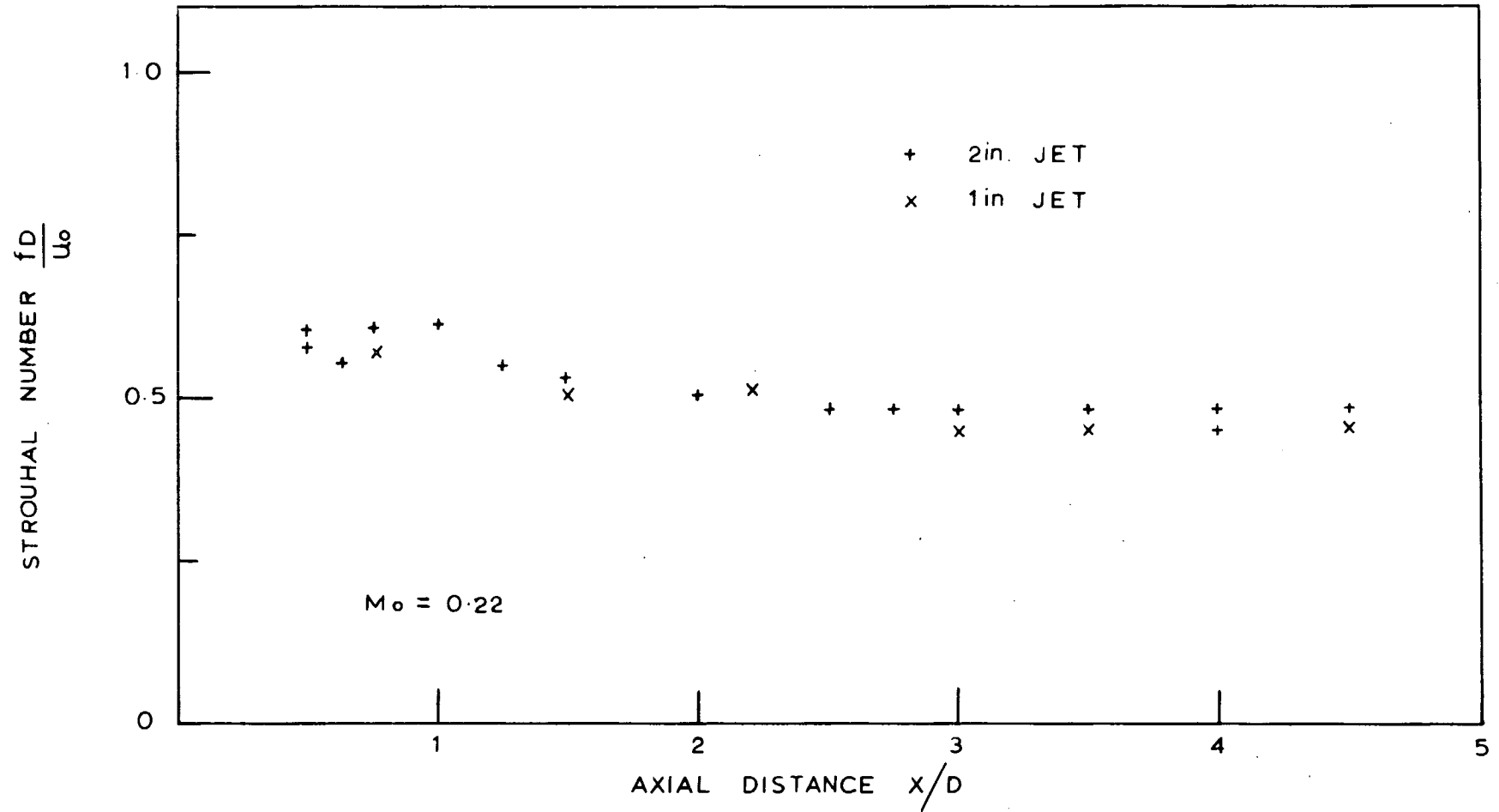


Fig. 4. Strouhal number of the hot wire signals in the potential core.

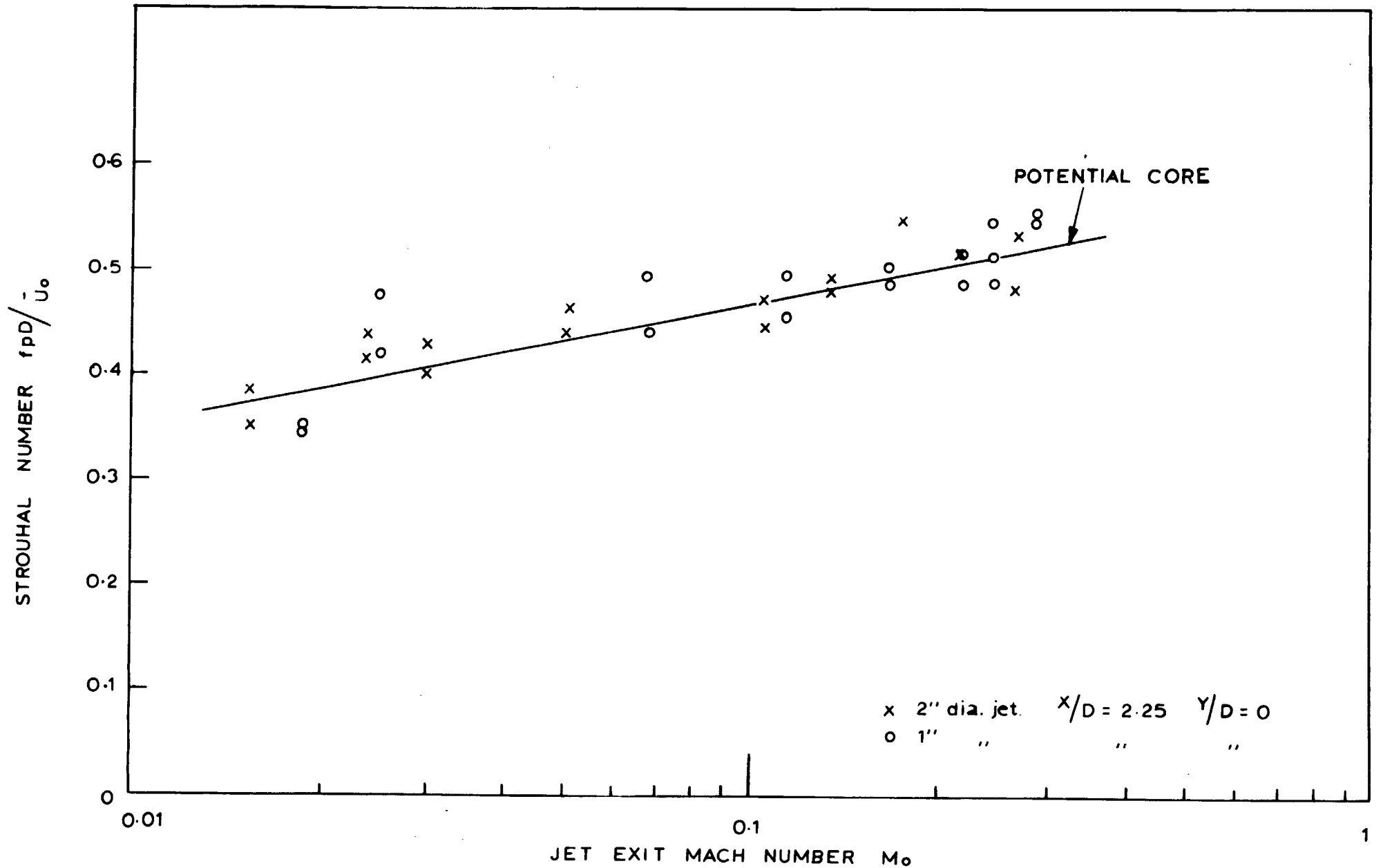


Fig. 5 Strouhal number against Mach number for different jets.

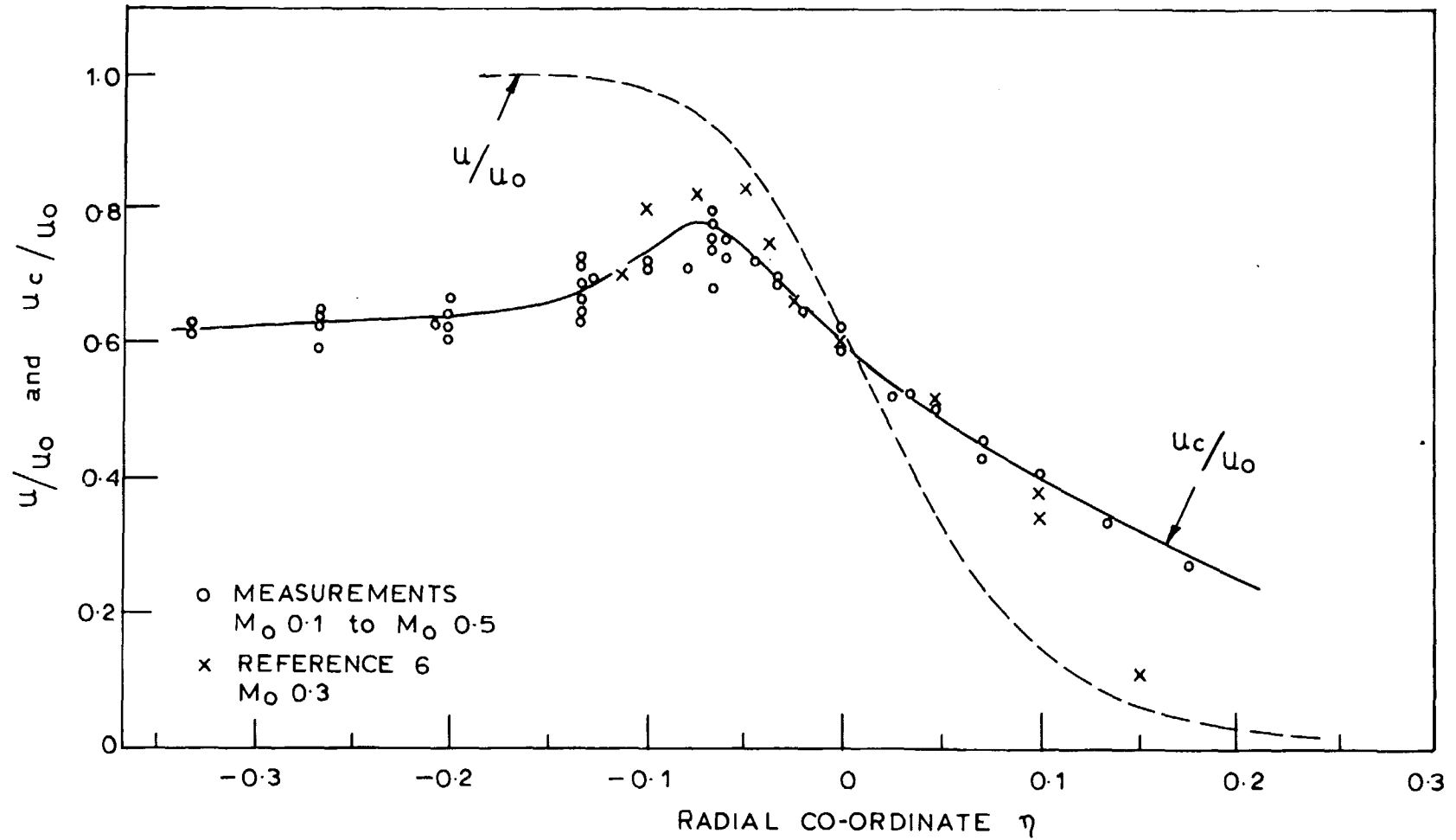


Fig.6. Radial distribution of axial convection velocity along rays $\eta = \text{const.}$

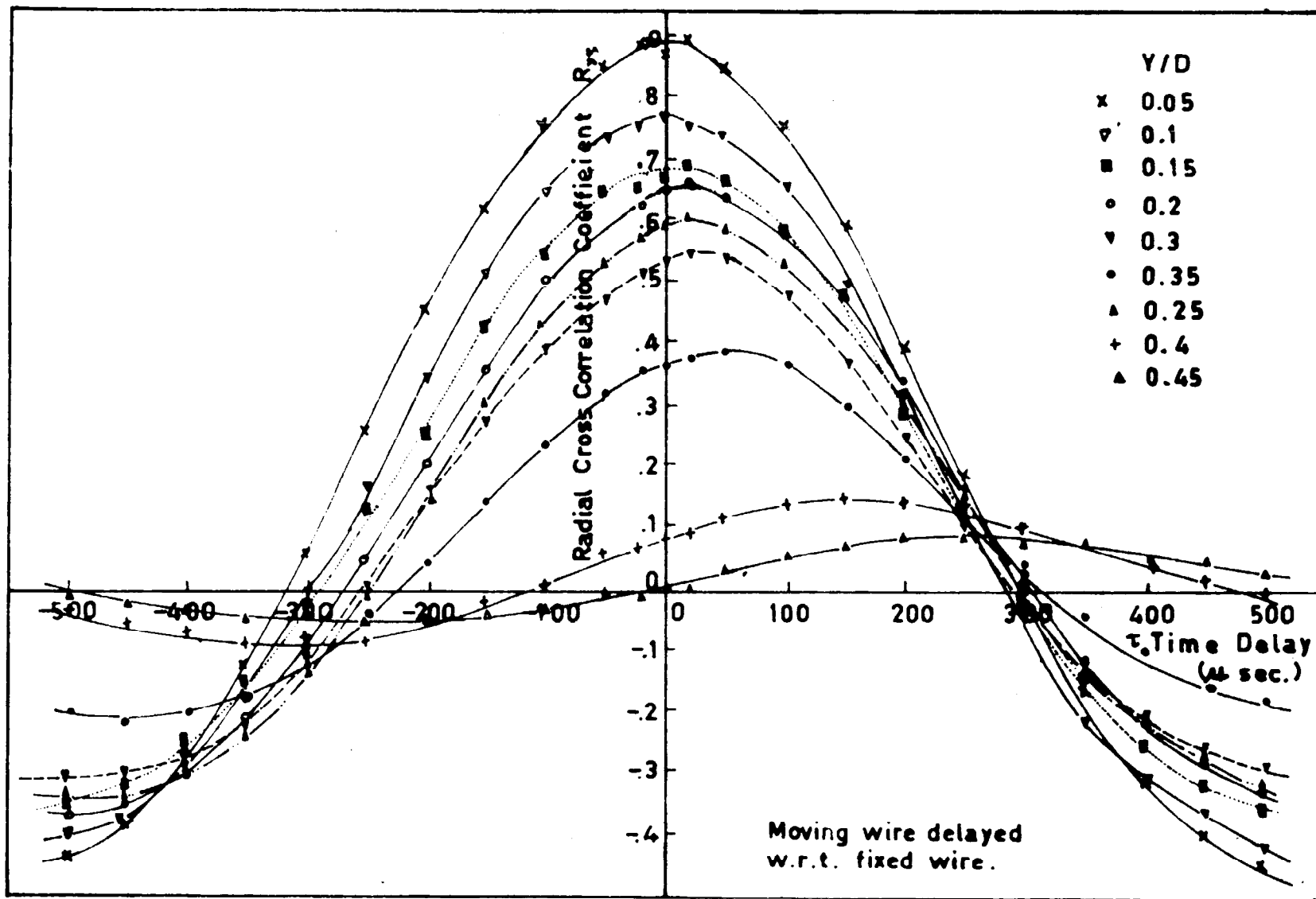


Fig.7 Radial Distribution of Cross Correlation Coefficient.
 Jet Dia. 2". F.W. at $X/D=1.5$. $Y/D=0$. $U_0=242$ ft/sec.

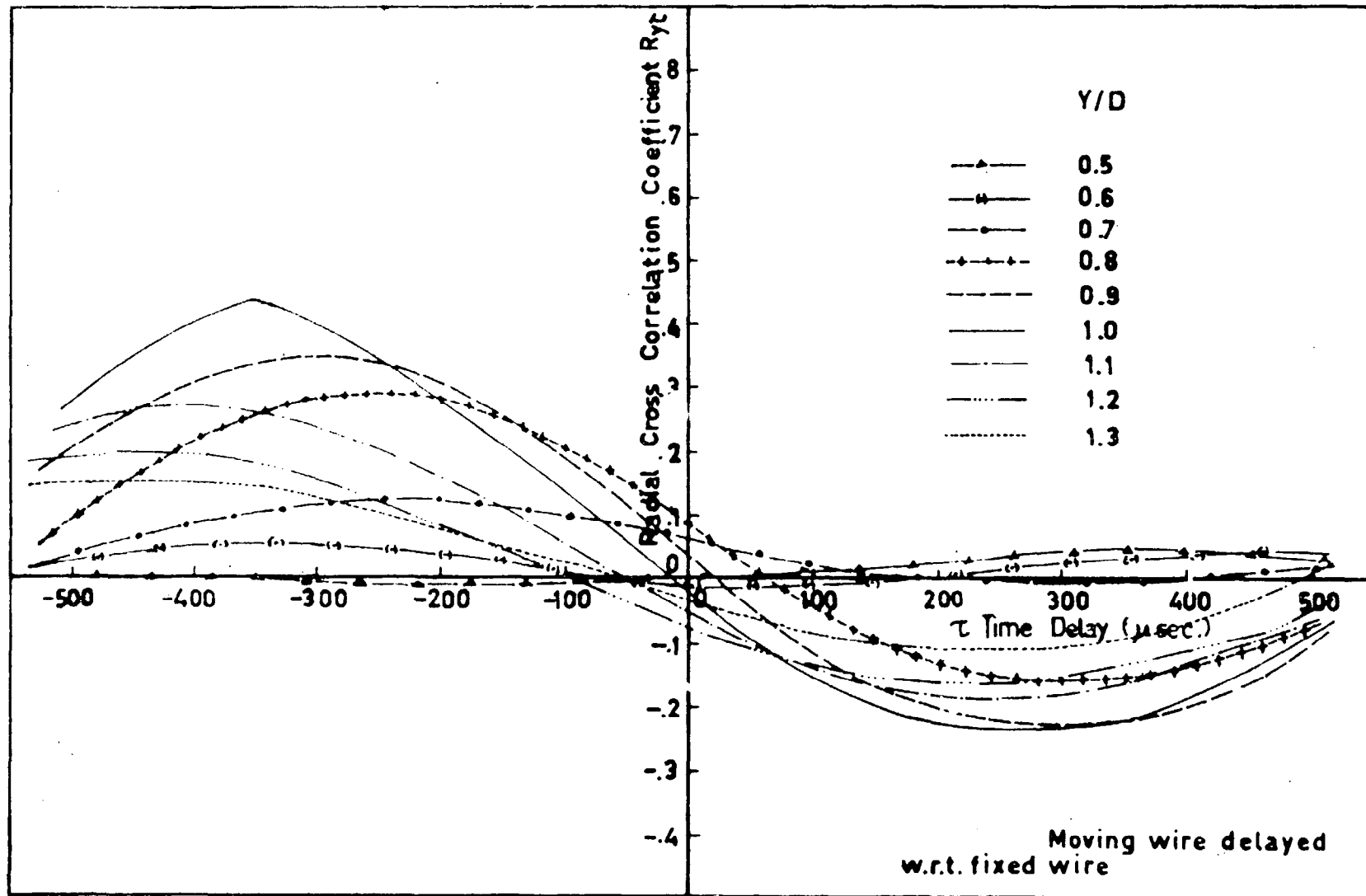


Fig. 8 Radial Distribution of Cross Correlation Coefficient.
 Jet Dia. 2". F.W. at $X/D=1.5$. $Y/D=0$. $\bar{U}_0=242$ ft/sec.

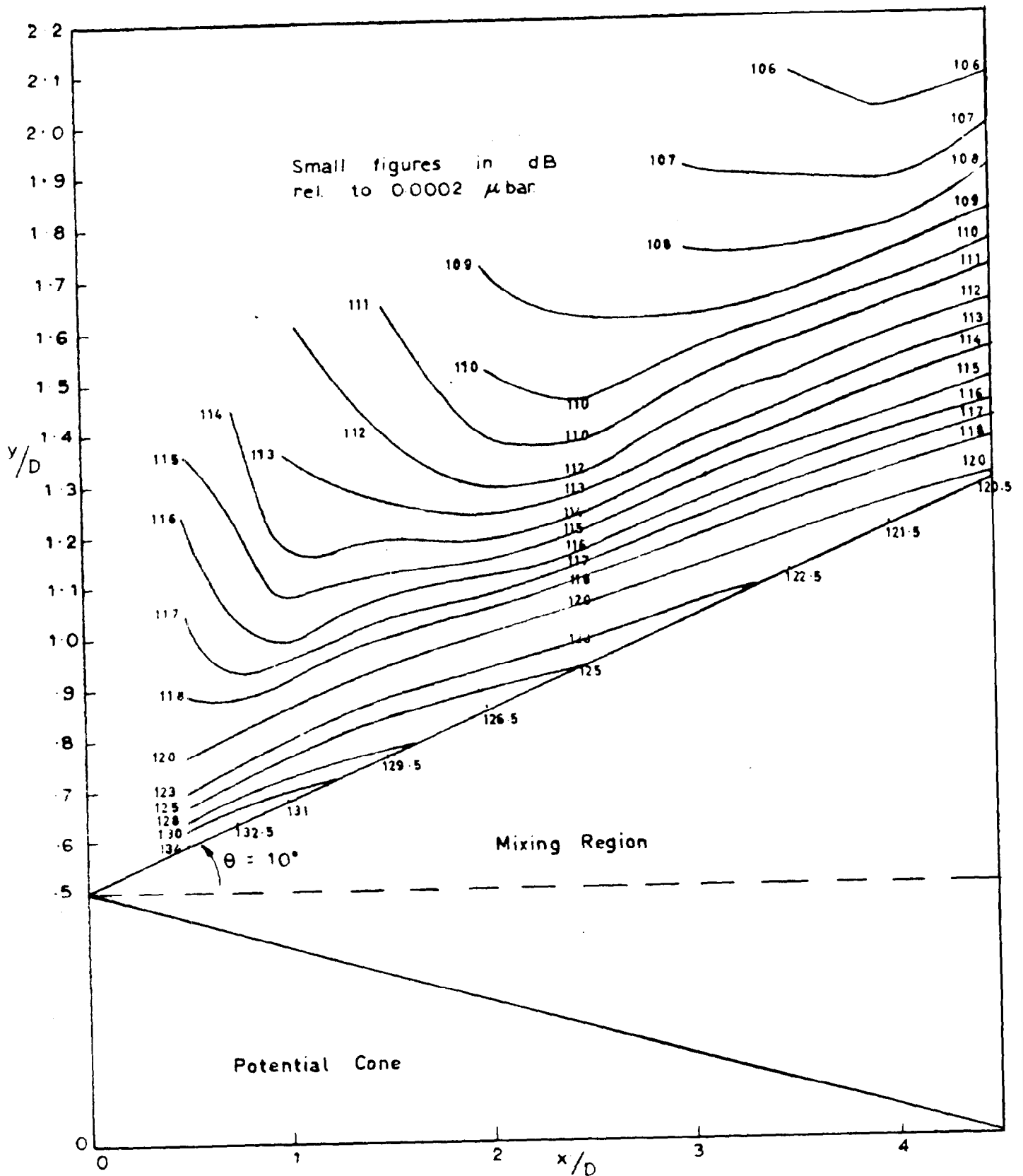


Fig 9. Pressure distribution of the near field.
Jet diameter 2" $\bar{U}_0 = 242$ ft /sec. $\frac{1}{4}$ " microphone.

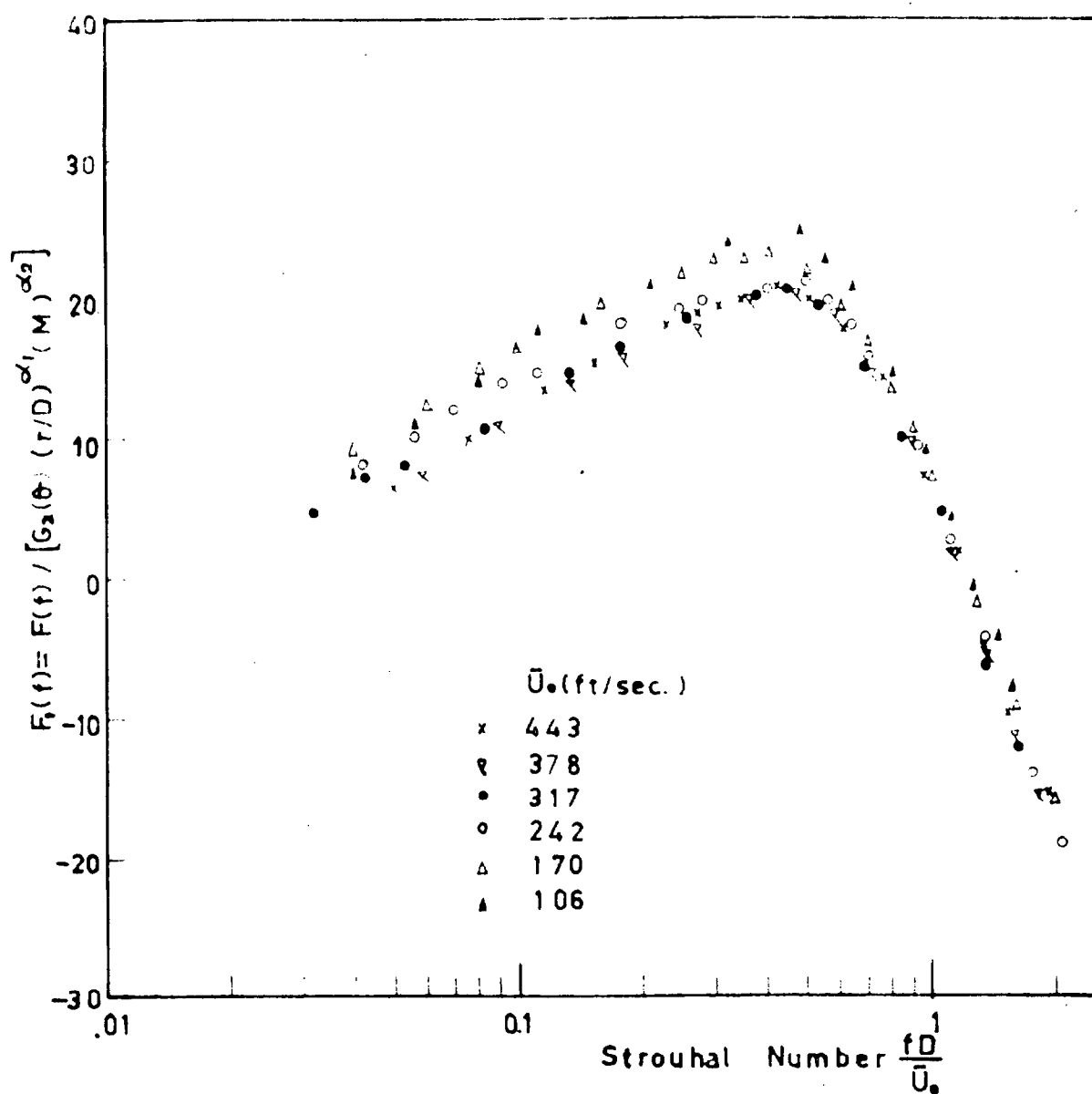


Fig. 10 Similarity in sound pressure spectra in the near field outside the jet.
 Jet dia. 2" X/D=2.25, $\theta=10^\circ$. 1/4 in. microphone.
 $\alpha_2 = 3.30$

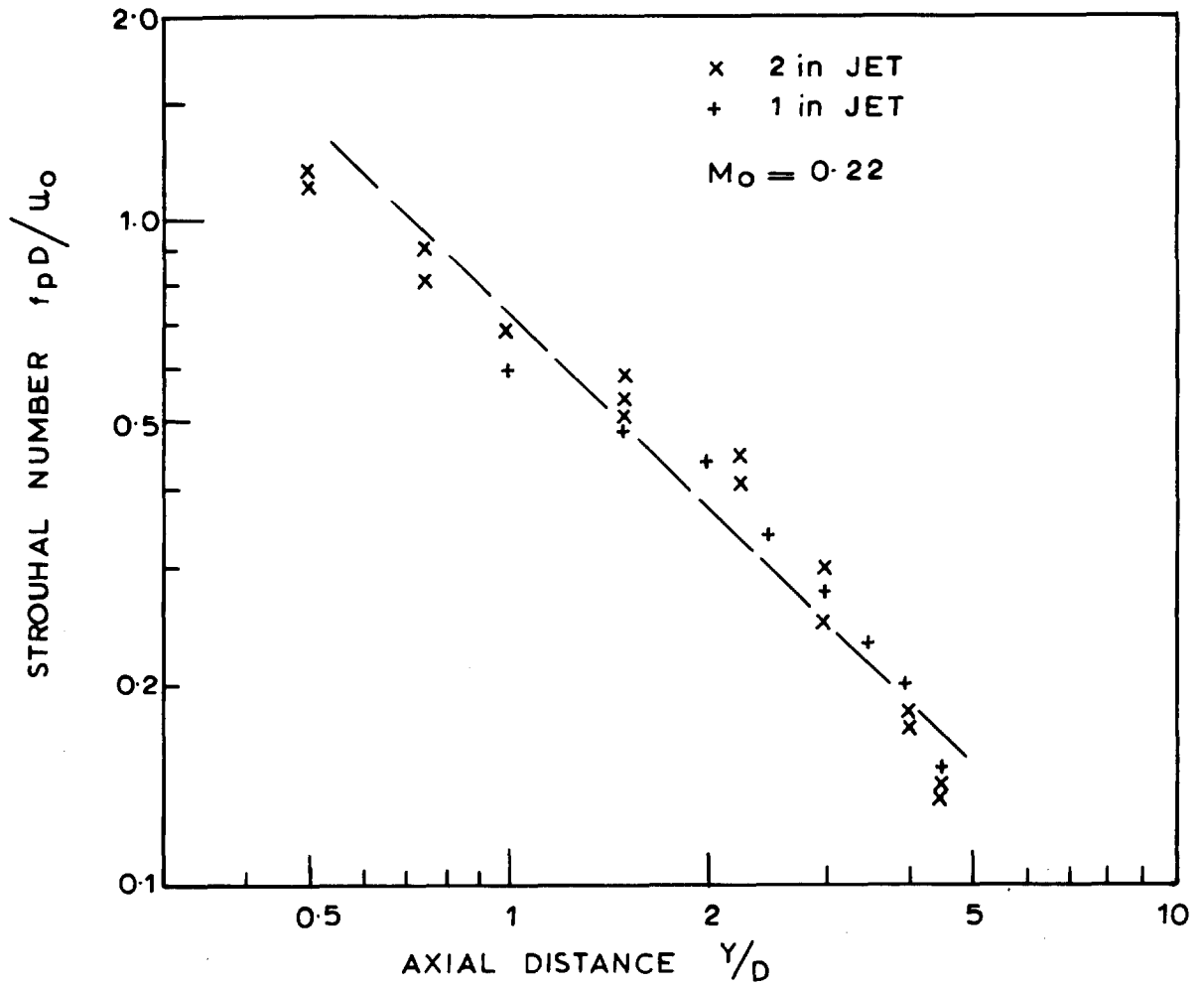


Fig.11. Axial variation of the pressure field frequency along the edge of a jet.

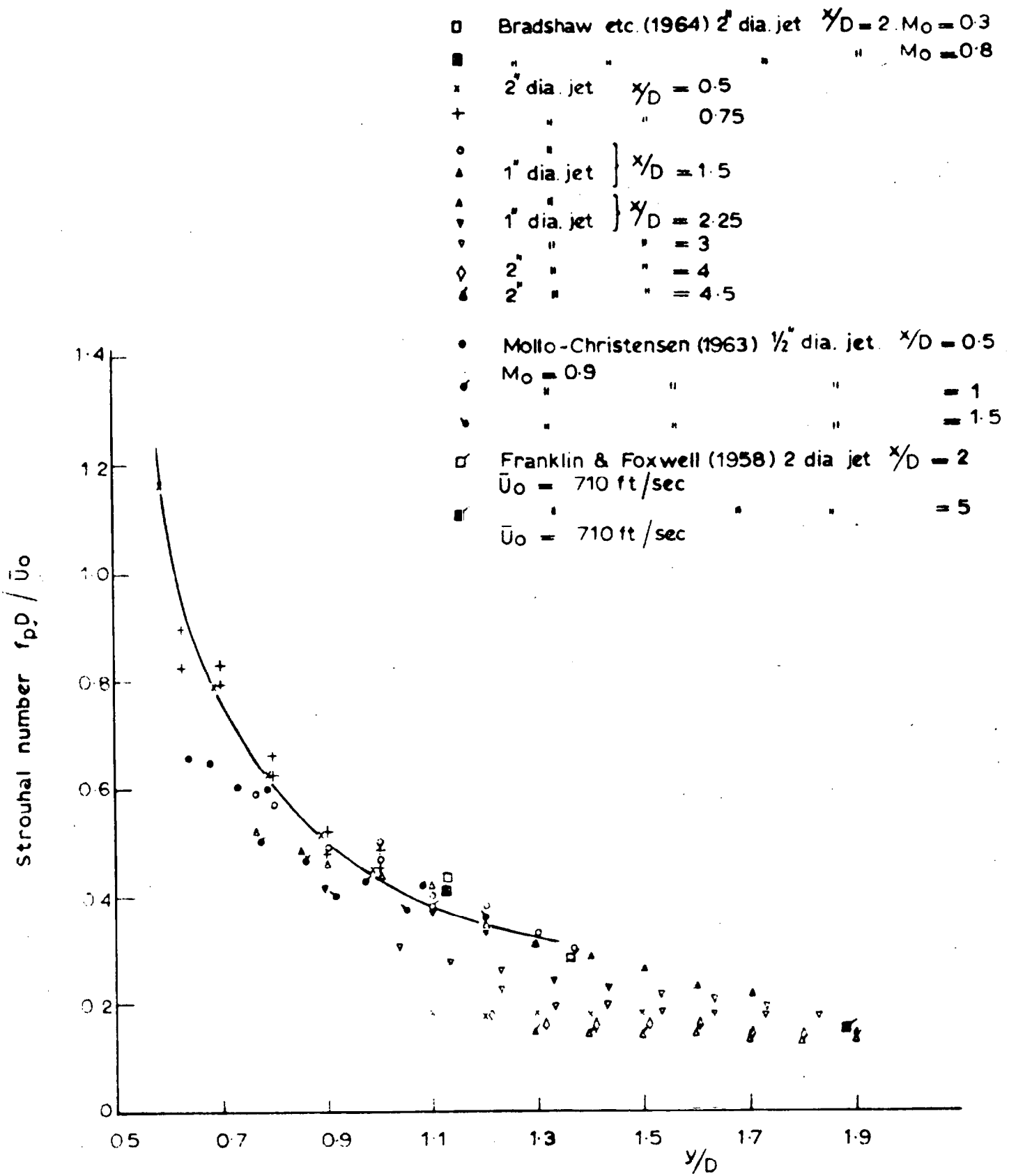


Fig-12 Radial distribution of the Strouhal number of the sound pressure spectra in the near field outside the jet. $\bar{U}_0 = 242$ ft/sec, $1/4$ " microphone.

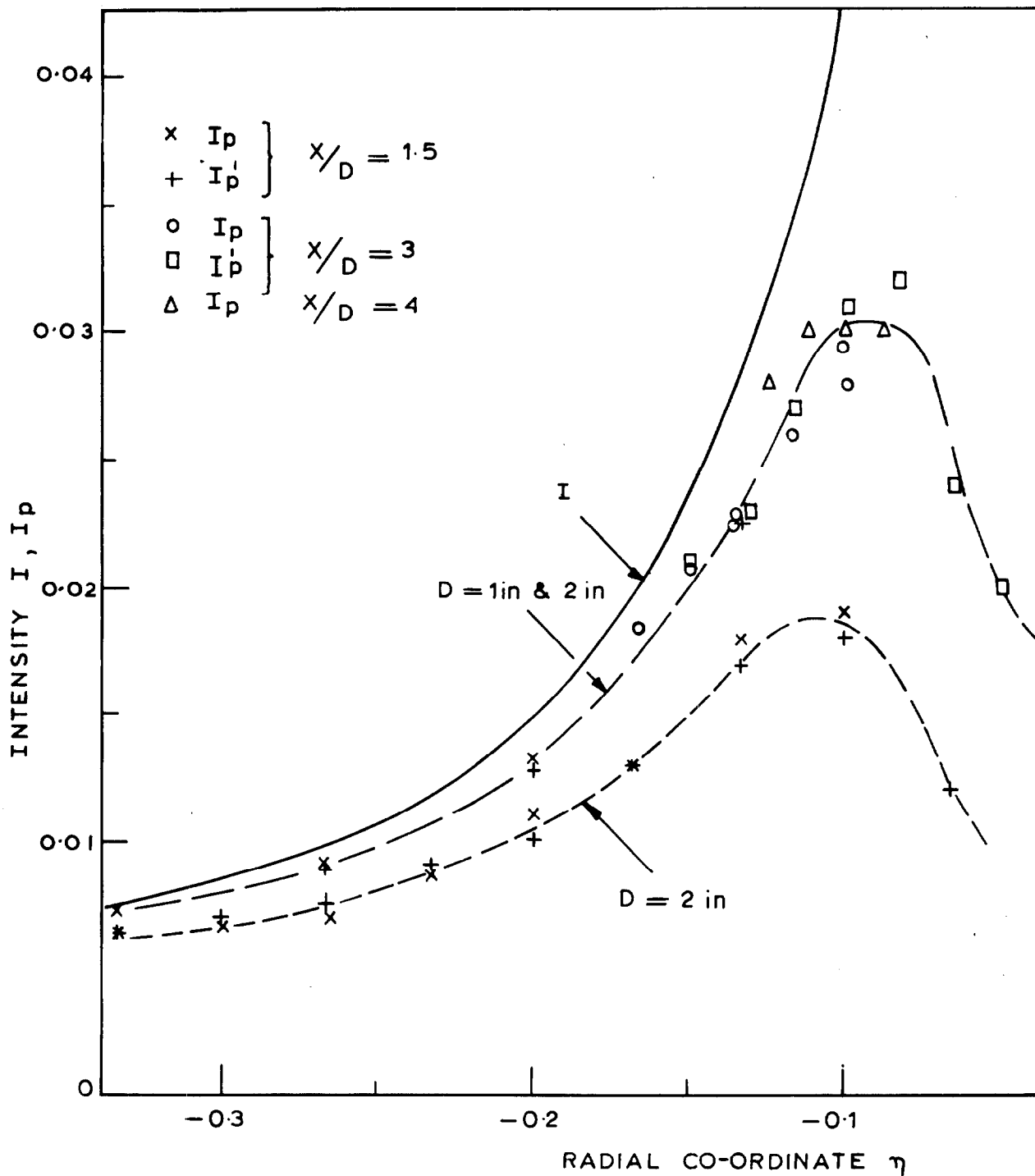


Fig. 13 . Estimates of the pressure field : intensity in and near the potential core .

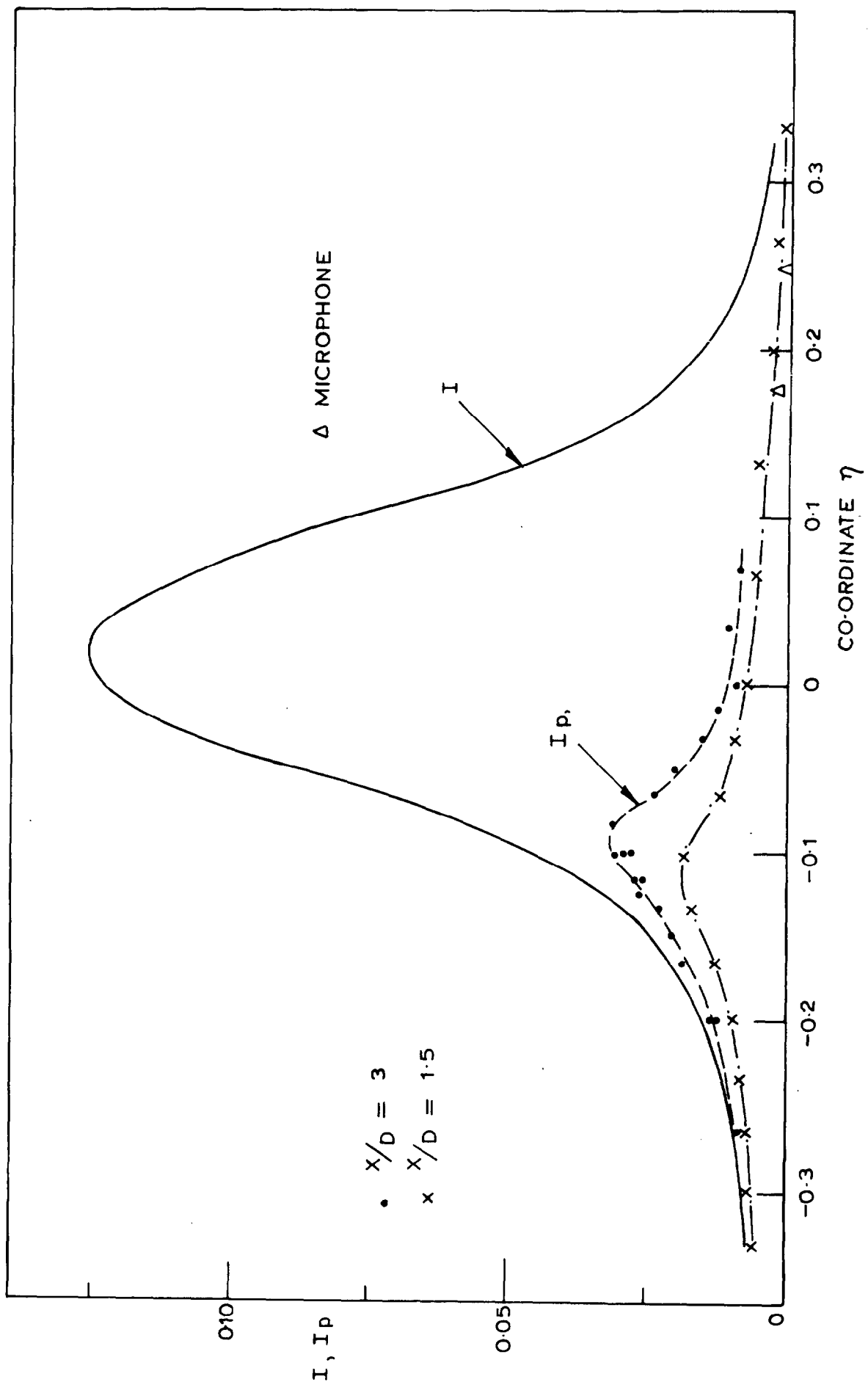


Fig. 14. Distribution of turbulent and pressure intensity.

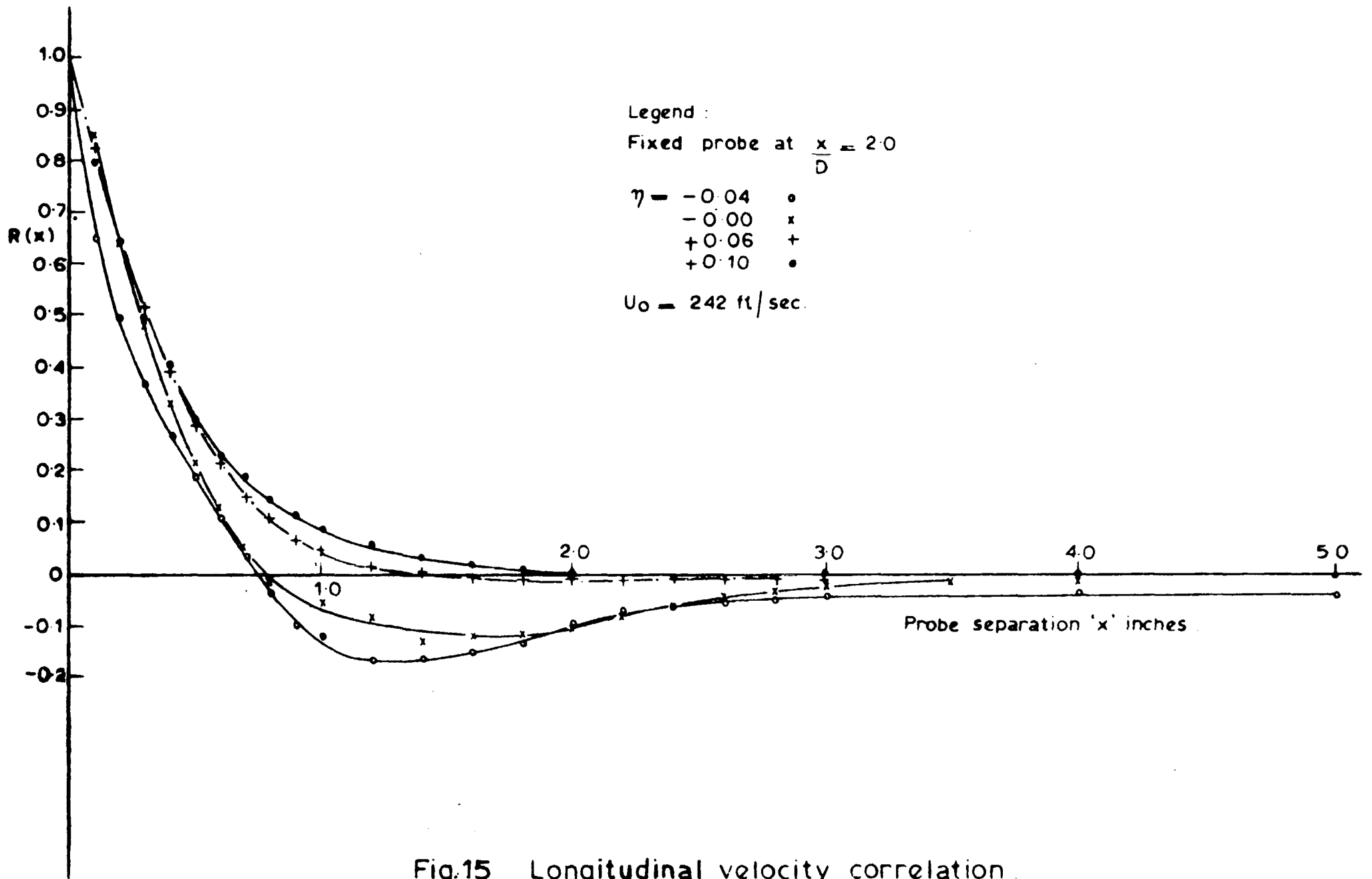


Fig.15. Longitudinal velocity correlation.

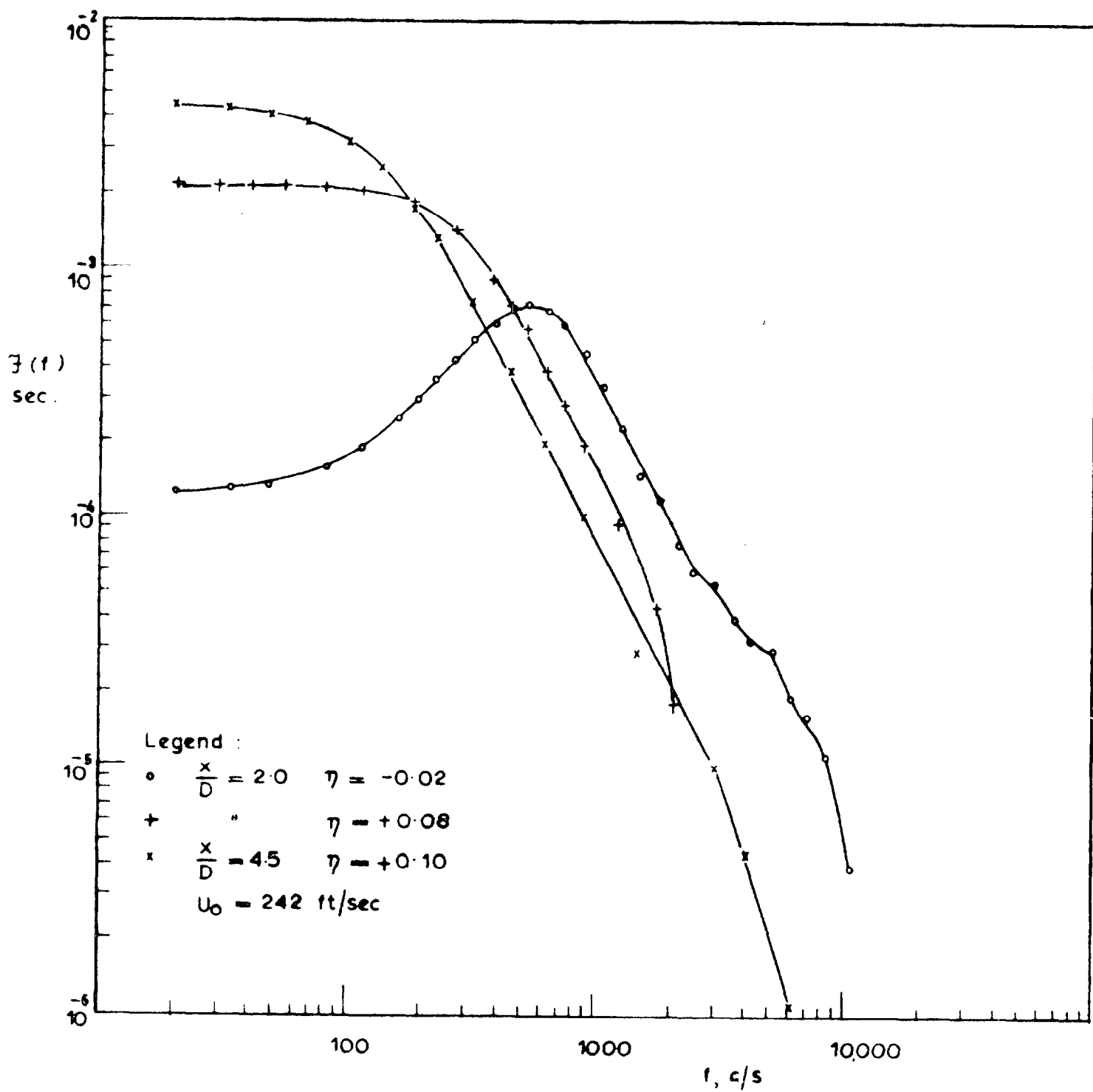


Fig.16. Spectral density from transform.

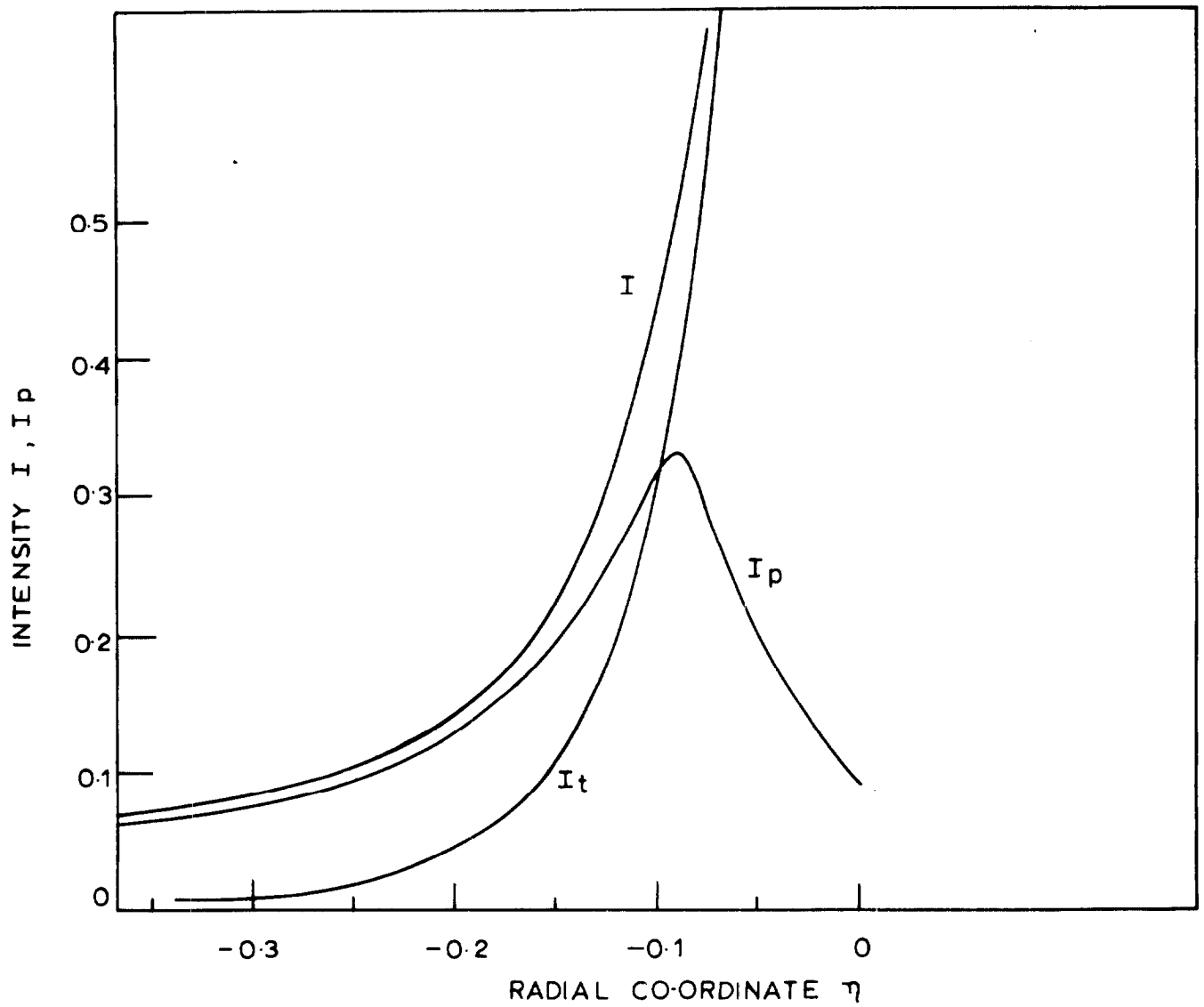


Fig. 17. Comparison of relative intensity of pressure and velocity fluctuations.

A.R.C. C.P. No. 989

May, 1967

P. O. A. L. Davies, N. W. M. Ko and B. Bose.

THE LOCAL PRESSURE FIELD OF TURBULENT JETS

The characteristics of the pressure field associated with the turbulent shear flows of a jet have been studied in some detail. Components of the field in the potential core appear to be moving with a phase velocity equal to the local speed of sound in directions roughly normal to the shear layer. Some components of the hot wire signal can be associated with the jet structure as a single complex source while others are related to the local characteristics of the turbulence.

An estimate of the strength of the fluctuating pressure field throughout the whole region of the jet flow is presented.

A.R.C. C.P. No. 989

May, 1967

P. O. A. L. Davies, N. W. M. Ko and B. Bose.

THE LOCAL PRESSURE FIELD OF TURBULENT JETS

The characteristics of the pressure field associated with the turbulent shear flows of a jet have been studied in some detail. Components of the field in the potential core appear to be moving with a phase velocity equal to the local speed of sound in directions roughly normal to the shear layer. Some components of the hot wire signal can be associated with the jet structure as a single complex source while others are related to the local characteristics of the turbulence.

An estimate of the strength of the fluctuating pressure field throughout the whole region of the jet flow is presented.

A.R.C. C.P. No. 989

May, 1967

P. O. A. L. Davies, N. W. M. Ko and B. Bose.

THE LOCAL PRESSURE FIELD OF TURBULENT JETS

The characteristics of the pressure field associated with the turbulent shear flows of a jet have been studied in some detail. Components of the field in the potential core appear to be moving with a phase velocity equal to the local speed of sound in directions roughly normal to the shear layer. Some components of the hot wire signal can be associated with the jet structure as a single complex source while others are related to the local characteristics of the turbulence.

An estimate of the strength of the fluctuating pressure field throughout the whole region of the jet flow is presented.

A.R.C. C.P. No. 989

May, 1967

P. O. A. L. Davies, N. W. M. Ko and B. Bose.

THE LOCAL PRESSURE FIELD OF TURBULENT JETS

The characteristics of the pressure field associated with the turbulent shear flows of a jet have been studied in some detail. Components of the field in the potential core appear to be moving with a phase velocity equal to the local speed of sound in directions roughly normal to the shear layer. Some components of the hot wire signal can be associated with the jet structure as a single complex source while others are related to the local characteristics of the turbulence.

An estimate of the strength of the fluctuating pressure field throughout the whole region of the jet flow is presented.

© *Crown copyright 1968*

Printed and published by
HER MAJESTY'S STATIONERY OFFICE

To be purchased from
49 High Holborn, London W.C.1
423 Oxford Street, London W.1
13A Castle Street, Edinburgh 2
109 St. Mary Street, Cardiff CF1 1JW
Brazennose Street, Manchester 2
50 Fairfax Street, Bristol 1
258-259 Broad Street, Birmingham 1
7-11 Linenhall Street, Belfast BT2 8AY
or through any bookseller

Printed in England